Journal of Biomechanics 87 (2019) 54–63

Contents lists available at ScienceDirect

Journal of Biomechanics

journal homepage: www.elsevier.com/locate/jbiomech
www.JBiomech.com

Model of loadings acting on the femoral bone during gait

Justyna Skubich *, Szczepan Piszczatowski

Bialystok University of Technology, Department of Biocybernetics and Biomedical Engineering, Bialystok, Poland

ARTICLE INFO

Article history:
Accepted 20 February 2019

Keywords:
Femur
Muscle force
Hip-joint force
Musculoskeletal model
Gait

ABSTRACT

An evaluation of the model of loadings acting on the femoral bone during the whole gait cycle was the main aim of the paper. A computer simulation of the musculoskeletal system based on the gait data collected during gait was used to determine the muscle forces as well as the hip joint reaction. Kinematic parameters as well as the ground reaction force for ninety-nine healthy persons of both sexes (18–36 years old) who had no history of musculoskeletal disease were registered during normal gait with preferred speed and used as inputs for musculoskeletal modelling and numerical simulation with the use of the AnyBody software. Time waveforms of the values of force generated by 21 muscles having attachments on the femoral bone as well as the hip joint reaction force were obtained. Directions of particular forces were presented using a femoral coordinate system. Attachment points for all muscle forces were obtained on the basis of the unscaled standard model with the length of the femur equal to 0.41 m. The presented model of loadings acting on the femoral bone element can be useful for the biomechanical analysis of bone development and remodelling as well as for the optimisation of implant or bone stabilizer design and pre-clinical testing.

1. Introduction

Mechanical loadings play an important role in the musculoskeletal system, its development and maintenance. In adults, mechanical stimuli are of paramount importance in the process of bone tissue remodelling leading to bone reinforcement or weakening in particular regions (Cowin and Hegadus, 1976; Prendergast 2002). A nonhomogeneous structure of the bone elements was found to be an outcome of this phenomenon (Jang and Kim, 2009; Machado et al., 2014). During childhood, when the bone development process is in progress, the growth plates are stimulated by mechanical loadings (Carter et al, 1996). As a result, the velocity of bone growth and the final outcome of such process, i.e. bone shape and dimensions, are dependent on loadings acting on the growing bone. Abnormal forces acting on particular bones may lead to pathological changes of bone shape and, in consequence, to a disturbance of the spatial structure of the whole skeleton (Piszczatowski, 2008). However, there are examples where appropriate mechanical conditions applied on a pathologically deformed bone element may lead to its straightening (Rauch, 2005). Moreover, it must be emphasised that not only the amplitude, but also the direction and the time-history of particular forces acting in the musculoskeletal system are important (Niinimäki et al., 2017). Mechanical loadings have also a great influence on the endurance of endoprostheses fixed within bone elements due to the risk of its aseptic loosening as a result of bone tissue atrophy or fatigue damage of the bone cement (Bitsakos et al., 2005; Jonkers et al., 2008). On the other hand, a stabilization used in fracture treatment must overcome external loadings acting on particular bone fragments (Märdian et al., 2015).

All situations described above indicate the importance of learning loadings acting on particular bone elements. A set of forces acting in the musculoskeletal system is a result of a balance between internal and external loading. In general, the unknowns in biomechanical analysis of particular part of the musculoskeletal system are the joint reaction forces and forces generated by muscles, whereas such activity is necessary to stabilize particular body parts or move them. There are various methodologies for determining loadings acting inside the musculoskeletal system. With regard to the hip joint region, one of the most important parts of the musculoskeletal system, the basic model of loadings was made by Pauwels (1976) who analysed forces acting in the hip joint on the femoral bone for standing on one leg or on both legs, based on anthropometric data published in 1900 by Fisher. The loading acting on the femoral head during standing on one leg was estimated at the level of 300% of the body weight (BW) whilst the muscle force acting on the greater trochanter was equal to about 244%BW. Similar analyses for the hip joint region are still used

* Corresponding author at: Wiejska 45C, 15-351 Bialystok, Poland.
E-mail addresses: j.skubich@pb.edu.pl (J. Skubich), s.piszczatowski@pb.edu.pl (S. Piszczatowski).

https://doi.org/10.1016/j.jbiomech.2019.02.018
0021-9290/

for the estimation of loadings acting in a single anatomical position, especially to analyse the influence of disturbed anatomical relation in the musculoskeletal system (Piszczatowski, 2008). Similarly, Bitsakos et al., (2005) in a simulation of remodelling of the proximal part of the femur, used a simple geometrical analysis for the estimation of muscle force direction taking into account the localization of muscle attachments on the femur and the pelvis. However, values of particular muscle forces were taken from an earlier research study of Duda (1996). The hip-joint reaction force (HJF) was measured experimentally by Davy et al. (1988) and evaluated at the level of 210%BW for standing on one leg and 266% for a gait with the use of crutches. A lesser value of HJF (238%BW) was obtained for normal walking of a patient with an implanted hip joint endoprosthesis by Bergmann et al. (2001). Kinematic data, collected parallelly to HJF measurements during gait, was a basis for the calculation of muscle forces using numerical simulations (Heller et al., 2001; Heller et al., 2005). The model of muscle forces acting on the femur obtained in this way was used later for a simulation of proximal femur adaptation (Machado et al., 2014). A similar methodology, i.e. numerical simulations based on the kinematic and kinetic data (ground reaction force) with the use of inverse dynamic analysis, was used to predict the loading acting on the femur and finally the hip joint contact forces by Lenaerts et al. (2008), Jonkers et al. (2008), Thielen et al. (2009), Seo et al. (2014) or Yadav et al. (2016). However, the abovementioned research studies were conducted for a single patient (adult or child) and the results of loadings acting on the femoral bone were limited to a few specific time-points in the gait cycle. Still, there is a lack of research with a similar analysis based on data collected for a large cohort of healthy, young people. Such results would be interesting as basic data useful for the comparison with results obtained for particular patients, especially in pathological conditions. Loadings acting on the femur, averaged for a quite large group of people, may be useful also for a variety of biomechanical analyses, e.g. simulations of bone development and remodelling, implant design process, forecasting of the probable course of pathological bone structure changes, etc.

In such situation, the aim of the research was to present a pattern of loadings acting on the femoral bone during normal gait, taking into account the hip-joint reaction force as well as the forces generated by muscles attached to the femur, based on kinematic and kinetic data registered for a large group of young, healthy persons.

2. Materials and methods

2.1. Participants

Ninety-nine healthy subjects of both sexes (18–36 years old), with no historical injuries or damages on the lower limbs at the time of the experiment were recruited for this study (Table 1). The study was approved by the Ethical Review Board.

2.2. Instrumentation and data collection

Twenty-four reflective skin markers were placed on the lower part of the body for each participant according to a modified Helen Hayes marker set (Davis et al., 1991). Additional markers placed on medial femoral epicondyles and medial malleoluses as well as three markers located on the foot were used to improve the movement recording of the distal part of the lower limb. Participants of the study walked along a 9-meter walkway at their preferred speed at least 10 times. The time-spatial trajectories of the markers were registered using the Qualisys Motion Capture system (Qualisys, Gothenburg, Sweden) consisting of 10 infrared cameras and 1 video camera. The ground reaction forces were measured simultaneously using two 600 × 500 mm force platforms (9260AA6, Kistler, Winterthur, Switzerland) embedded in the floor of the laboratory and placed one after the other with 5 mm gap. Marker data were registered at the frequency of 118 Hz and analogue data from the force platforms at 1298 Hz.

2.3. Musculoskeletal model and inverse dynamics analysis

The musculoskeletal model used for the analysis was taken from a repository of the AnyBody Modeling System v.7.0 (AnyBody Technology, Aalborg, Denmark). The model consisted altogether of 12 body segments (head-trunk, pelvis, right and left: femur, patella, tibia, talus and foot) joined with the use of 11 joints providing 21 degrees of freedom. All segments were modelled as rigid bodies. The hip was modelled as a ball-and-socket joint with three degrees of freedom. The Hill's model used for the analysis of muscles consisted of contractile and elastic elements arranged in parallel and in series (Heinen et al., 2016). The model of each lower limb contained 56 muscles of which 21 had their attachments located on the each femoral bone (Klein-Horsman et al., 2007). Particular muscles were divided into actons with regard to their size, biomechanical function and localization of their attachments on the bones, etc. For example, *gluteus maximus* and *medius* were divided into two actons (superior/inferior or anterior/posterior) due to their different anatomical functions and attachment areas. Finally, the muscular model of each lower limb, in accordance with the original TLEM dataset, consisted of 159 branches of which 123 had their attachments located on the each femoral bone (Klein-Horsman et al., 2007).

Anthropometric data were used to scale the model for individual persons and to determine bone dimensions and inertial parameters according to the Length–Mass–Fat scaling law (Rasmussen et al. 2005, Lund et al., 2015). Furthermore, times-spatial trajectories of markers, recorded for each subject, were used to optimize the pelvis width as well as the thigh, shank and foot lengths, using the parameter identification algorithm. The location of muscle attachment was scaled together with the whole model. The individually scaled model, together with experimentally 101 recorded time-spatial trajectories of markers and the ground reaction force (filtered using a second-order forward-backward low-pass Butterworth filter, with cut-off frequencies of 5 Hz and 12 Hz respectively) provided input data for musculoskeletal modelling with the use of inverse dynamics analyses. The muscle forces were determined using the numerical optimization procedure with the polynomial, third power muscle recruitment criterion (Damsgaard et al., 2006). The choice of the optimization criterion was made on the basis of the recommendation of Prilutsky and

Table 1
Characteristics of the study group (mean ± SD).

	Group size	Age (year)	Weight (kg)	Height (cm)
Women	54	23.63 ± 3.03	61.21 ± 7.61	166.68 ± 6.31
Men	45	26 ± 5.46	80.78 ± 10.52	180.39 ± 6.06
Total	99	24.70 ± 4.51	70.14 ± 13.36	172.99 ± 9.26

Gregor (2000), Prilutsky and Zatsiorsky (2002) and Erdemir et al. (2007).

In this way the resultant hip joint force as well as the muscle forces for each acton attached to the femoral bone were obtained. All results were calculated relative to the femoral coordinate system defined for the right femur in accordance to its position during gait (Fig. 1) in agreement with the recommendation of the International Society of Biomechanics (ISB) (Wu et al., 2002). Data from left femur were mirrored to the right side.

2.4. Methodology for analysis of forces acting on the femur

The values of muscle forces and hip-joint reaction as well as their standard deviations were normalized by the body weight (% BW). The time characteristics of particular forces were adjusted to the duration of the gait cycle (GC) (time between two consecutive heel-strike events of the analysed limb). The results obtained in all correct trials were averaged for each participant. The subject average results were used to calculate an average result for the whole group.

In order to obtain a realistic, but at the same time functional and easy-to-use model of loadings acting on the femoral bone, the process of aggregation of results obtained for particular parts of muscles was carried out. The localization of particular acton's attachment in the AnyBody model as well as the timing of their activity during the gait cycle were analysed before deciding about summing up forces generated by particular parts of the muscles. As a result, all 123 abovementioned branches of muscles acting on the femoral bone were grouped forming a final muscle model consisting of 28 actons (Table 2). Taking into consideration fact, that all branches of analysed actons were attached to the rigid model of the femoral bone, the resultant forces for particular actons were obtained summing up vectors of the all muscle forces obtained for particular branches. In practice, the values of muscle force components generated by particular muscle branches included in the certain actons were summed up to obtain the final value of force generated by the whole acton in particular directions. Based on these components, the value of resultant muscle force generated by particular actons was calculated. In order to present direction of the resultant force vector, the angles of its deviation (Fig. 1) from the sagittal α (+α - laterally; -α - medially) and coronal β (+β - anteriorly; -β - posteriorly) planes of the femur were calculated.

3. Results

3.1. Hip-joint reaction force

The resultant hip-joint reaction force (HJF) acting during the gait cycle on the femoral head and its three components in the femoral coordinate system are presented in Supplementary Table 1 and Fig. 2. The waveforms of the resultant force as well as both proximo-distal (P-D) and medio-lateral (M-L) components have a characteristic profile with two pronounced local maxima separated by a local minimum. It can be noticed that the first maximum (the highest value during a gait cycle) was related to the end of the loading response phase of the analysed limb (16%GC) whilst the second was related to the push-off phase (47%GC). The average values of resultant force maxima reached 404%BW and 322.6%BW, respectively. The average value of the minimum was equal to 182.9%BW and occurred at about 30%GC, which corresponded to the mid-swing phase for the contra-lateral foot. More detailed information regarding the value of the hip-joint reaction force was presented in Table 3 for eight specific time-points in the gait cycle (marked in Fig. 2, Supplementary Material), selected using a similar methodology as Duda et al. (1998) and Bitsakos et al. (2005).

Quite large variability of the hip joint reaction force at certain time intervals is related to the variability in the ground reaction force (GRF) measured by the force platforms (Fig. 3).

3.2. Muscular forces

As a result of numerical studies, the active force generated by all 28 muscles or their parts (listed in Table 2) having their

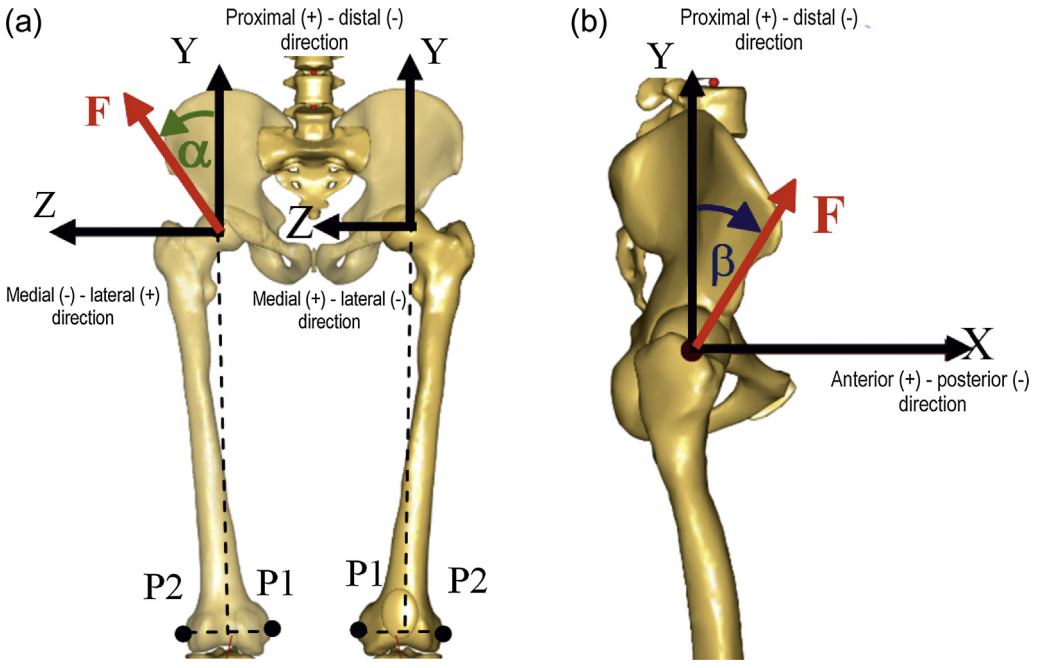

Fig. 1. The coordinate system connected with the right femoral bone; X - anterior (+)/posterior (-) direction; Y - proximal (+)/distal (-) direction; Z - lateral (+)/medial (-) direction; α - the angle of deviation of the force direction from the sagittal plane of the femur; β - angle of deviation of the force direction from the coronal plane of the femur: a) front view; b) right side view.

Table 2
Set of muscles or their parts acting on the femoral bones.

Muscle name	Abbrev.	Actons modelled in AnyBody	Muscle name	Abbrev.	Actons modelled in AnyBody
Gluteus Medius Posterior	GMeP	Gluteus Medius Posterior 1–6	Adductor Longus	AL	Adductor Longus 1–6
Gluteus Medius Anterior	GMeA	Gluteus Medius Anterior 1–6	Adductor Brevis	AB	Adductor Brevis Prox. 1–2 Adductor Brevis Distal 1–2 Adductor Brevis Mid. 1–2
Gluteus Minimus	GMi	Gluteus Min. Post. 1 Gluteus Min. Ant. 1 Gluteus Min. Mid. 1	Adductor Magnus Distal	AMD	Adductor Mag. Dis. 1–3
Gluteus Maximus Inferior	GMaI	Gluteus Max. Inferior 1–6	Adductor Magnus Middle	AMM	Adductor Mag. Mid 1–6
Gluteus Maximus Superior	GMaS	Gluteus Max. Superior 1–6	Adductor Magnus Proximal	AMP	Adductor Mag. Prox. 1–4
Obturator Internus	OI	Obturator Internus 1–3	Biceps Femoris Caput Breve	BF	Biceps Femoris Caput Breve 1–3
Obturator Externus	OE	Obturator Externus Inf. 1–2 Obturator Externus Sup. 1–3	Psoas Major	PM	Psoas Major 1–11
Piriformis	Pr	Piriformis 1	Iliacus	Il	Iliacus Lat. 1–3 Iliacus Mid 1–3 Iliacus Med. 1–3
Gemellus	Ge	Gemellus Sup. 1 Gemellus Inf. 1	Gastrocnemius Medialis	GM	Gastrocnemius Med. 1
Vastus Lateralis Superior	VLS	Vastus Lat. Sup. 1–2	Gastrocnemius Lateralis	GL	Gastrocnemius Lat. 1
Vastus Lateralis Inferior	VLI	Vastus Lat. Inf. 1–6	Popliteus	Po	Popliteus 1–2
Vastus Intermedius	VI	Vastus Intermedius 1–6	Quadratus Femoris	QF	Quadratus Femoris 1–4
Vastus Medialis Superior	VMS	Vastus Med. Sup. 1–6	Pectineus	Pe	Pectineus 1–4
Vastus Medialis Inferior	VMI	Vastus Med. Inf. 1–2 Vastus Med. Mid 1–2	Plantaris	Pl	Plantaris 1

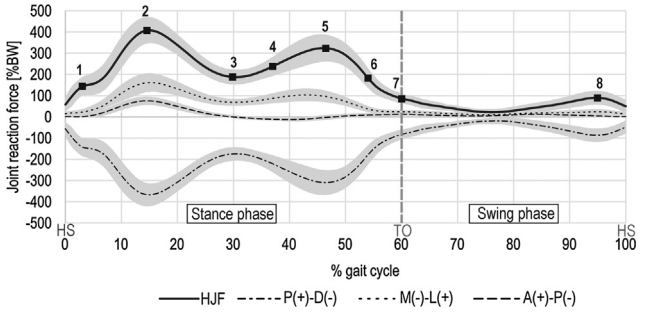

Fig. 2. The resultant hip-joint reaction force (HJF) acting on the femoral head and its components (M-L – medio (-)/lateral (+), A-P – antero (+)/posterior (-), P-D – proximo (+)/distal (-)) expressed as percentage of body weight (%BW) through the gait cycle (mean ± SD); TO - toe off, HS - heel strike.

attachments located on the femoral bone were determined (Supplementary Table 2). The results obtained for 24 actons are presented in graphical form (Fig. 4), omitting those muscles that generated forces of negligible value. The numerical results, calculated for the eight abovementioned time-points, for all muscles are shown in Table 4.

In approximately half of the actons, muscle force had a time waveform similar to the hip joint reaction force with two characteristic local peaks at about 16%GC and 47%GC. This group included hip abductors, in particular *gluteus medius* and *minimus*, knee extensors, e.g. *vastus* muscles, psoas and external hip rotators, e.g. OI, Pr, Ge. Although for all these muscles two local maxima at about 16%GC and 47%GC may be observed, the proportions between the values of individual muscle forces generated at

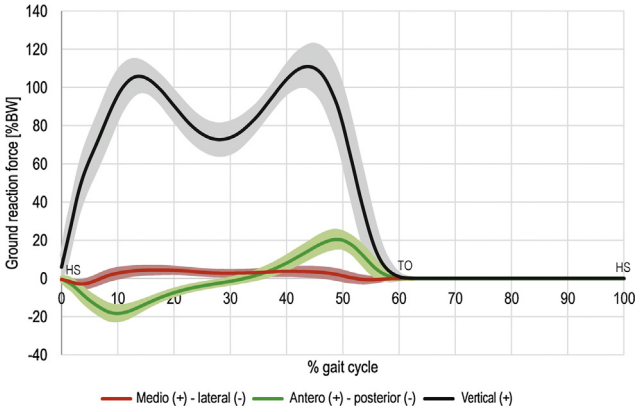

Fig. 3. The ground reaction force (GRF) expressed as percentage of body weight (%BW) through the gait cycle (mean ± SD); TO - toe off, HS - heel strike.

Table 3
Values of resultant hip-joint reaction force and its components for 8 selected time-points during the gait cycle (time-points in accordance with Fig. 2); A-P - anterior (+)/posterior (-); P-D - proximal (+)/distal (-); M-L - medial (-)/ lateral (+).

	Hip-joint reaction force, mean value ± SD (%BW)			
Time-point number	Resultant HJF	Proximo-distal (P-D)	Medio-lateral (M-L)	Antero-posterior (A-P)
1	150.8 ± 44.6	−148.1 ± 43.3	27.8 ± 15.9	3.8 ± 7.6
2	404.0 ± 55.8	−363.4 ± 49.5	160.6 ± 40.0	73.6 ± 17.2
3	188.0 ± 32.5	−174.9 ± 29.4	68.9 ± 14.6	−0.1 ± 6.4
4	237.8 ± 42.8	−220.8 ± 37.4	87.7 ± 21.6	−11.0 ± 4.7
5	322.6 ± 59.9	−308.7 ± 55.4	93.7 ± 24.4	−1.2 ± 9.2
6	182.9 ± 42.2	−178.9 ± 41.4	37.2 ± 12.1	9.1 ± 6.9
7	87.3 ± 21.0	−83.0 ± 21.2	23.9 ± 6.8	12.1 ± 4.5
8	90.1 ± 30.3	−86.8 ± 29.6	24.0 ± 9.8	4.6 ± 6.0

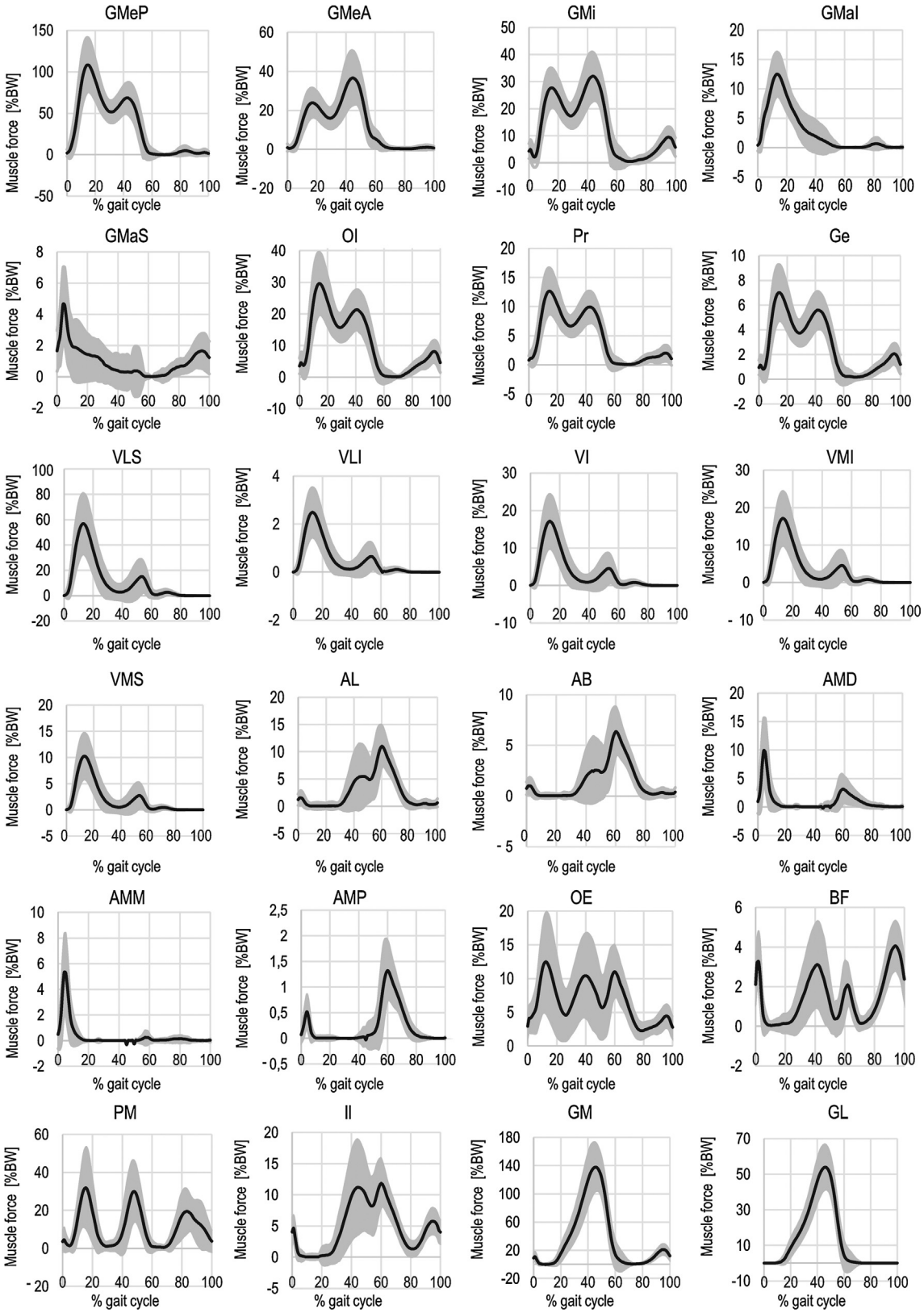

Fig. 4. Time waveforms of resultant muscle force for 24 actons acting on the femoral bone (mean ± SD) (abbreviations in Table 2).

particular time-points were different. Therefore, it is worth noting the difference in the action of posterior and anterior parts of the *gluteus medius*. While GMeP generated the maximum force at 16%GC, GMeA generated the maximum at 47%GC. In the case of the force generated by particular parts of *vastus* muscles, the second local maximum was much lower than the first and occurred

Table 4
Values of muscle forces and angles of their deviation from the sagittal; (-α - medially; +α - laterally) and coronal (-β - posteriorly; +β - anteriorly) planes of the femur for 8 selected time-points during the gait cycle (designations in Table 2 and Fig. 1).

Acton	(1) 4% gait cycle			(2) 16% gait cycle			(3) 30% gait cycle			(4) 37% gait cycle		
	F(%BW)	α (°)	β (°)	F(%BW)	α (°)	β (°)	F(%BW)	α (°)	β (°)	F(%BW)	α (°)	β (°)
GMeP	16.9	−35.4	33.7	106.9	−36.5	26.1	52.1	−32.5	9.1	59.6	−32.0	0.7
GMeA	1.3	−36.1	56.3	23.7	−32.2	48.9	16.1	−23.6	33.5	25.2	−20.1	25.3
GMi	2.2	−31.8	20.8	27.8	−32.0	18.0	17.7	−27.1	5.4	25.5	−25.4	−0.5
GMaI	4.8	−32.6	−15.4	11.7	−39.4	−18.9	3.8	−43.2	−26.1	2.3	−46.3	−28.2
GMaS	4.7	−13.8	−4.5	1.7	−15.4	−5.3	1.0	−14.7	−8.5	0.5	−15.1	−9.9
OI	4.5	−64.4	−57.7	28.8	−71.8	−66.3	15.8	−83.0	−81.3	20.0	−88.9	−88.7
OE	4.8	−82.2	−76.8	10.9	−89.0	−88.4	5.9	−104.9	−121.1	9.9	−109.6	−136.1
Pr	1.9	−48.6	−20.4	12.4	−55.1	−29.0	6.7	−60.2	−46.7	8.6	−64.8	−55.3
Ge	0.9	−63.3	−54.9	6.8	−69.7	−62.7	3.8	−80.8	−78.7	5.0	−87.6	−87.1
VLS	8.6	−171.0	−171.5	52.1	−171.0	−171.3	7.6	−170.8	−171.2	3.0	−170.5	−171.0
VLI	0.4	−172.2	−158.6	2.3	−172.3	−158.8	0.3	−172.1	−158.3	0.1	−171.8	−157.8
VI	2.6	−173.7	−169.0	15.7	−173.8	−168.9	2.3	−173.6	−168.7	0.9	−173.4	−168.5
VMI	2.7	−177.4	−156.1	16.2	−177.6	−156.6	2.4	−177.4	−155.9	0.9	−177.3	−155.5
VMS	1.6	−169.4	−166.8	9.4	−169.9	−166.7	1.4	−170.8	−166.5	0.5	−171.2	−166.2
AL	1.1	−24.1	−1.9	0.1	−26.0	8.3	0.2	−21.0	12.4	2.9	−20.7	12.8
AB	0.8	−52.3	0.1	0.0	−52.7	21.1	0.1	−50.7	33.9	1.1	−49.8	33.7
AMD	9.9	1.2	−11.4	0.2	2.4	−12.0	0.0	−4.9	−6.0	0.0	0.0	−8.0
AMM	5.3	−10.4	−21.3	0.1	−12.6	−24.8	0.0	−15.7	−14.9	0.0	−14.6	−19.4
AMP	0.5	−32.3	−25.4	0.0	−44.0	−7.0	0.0	−43.6	−14.1	0.0	−40.8	11.1
BF	1.5	−172.1	−178.1	0.1	−172.5	−178.8	1.2	−172.2	−178.7	2.6	−172.2	−178.7
PM	1.6	−29.8	42.3	31.7	−27.8	44.2	1.2	−21.6	39.7	3.1	−15.4	36.5
Il	0.7	−25.8	40.9	0.1	−19.8	35.4	2.3	−18.6	37.2	7.5	−17.3	36.6
GM	1.5	−170.3	−147.5	3.5	−170.1	−145.9	55.4	−170.3	−147.3	99.6	−170.0	−147.4
GL	0.0	−161.6	−118.3	3.1	−164.9	−118.8	22.4	−163.7	−118.9	38.4	−163.3	−119.0
Po	0.1	−118.2	−120.4	0.7	−114.6	−115.1	0.1	−118.0	−119.7	0.0	−119.2	−121.3
QF	2.2	−71.1	−56.5	0.9	−67.7	−53.5	0.7	−95.7	−118.6	1.8	−100.7	−152.2
Pe	0.2	−55.0	30.5	0.0	−48.8	30.0	0.2	−46.5	37.0	1.0	−44.8	36.5
Pl	0.0	−179.7	−168.6	0.2	−178.9	−154.1	0.5	−179.0	−162.9	0.7	−179.1	−165.9
Acton	(5) 47% gait cycle			(6) 54% gait cycle			(7) 60% gait cycle			(8) 95% gait cycle		
	F(%BW)	α (°)	β (°)	F(%BW)	α (°)	β (°)	F(%BW)	α (°)	β (°)	F(%BW)	α (°)	β (°)
GMeP	61.6	−31.2	−96.7	17.4	−28.7	−95.8	1.1	−28.1	−94.5	2.3	−36.3	24.7
GMeA	35.5	−18.4	18.8	15.7	−17.5	20.6	5.5	−17.5	27.3	1.1	−39.5	56.3
GMi	30.3	−24.2	−5.5	12.8	−22.5	−4.0	2.4	−19.5	4.4	9.5	−32.5	26.4
GMaI	1.0	−49.4	−31.6	0.2	−47.4	−30.5	0.0	−42.3	−32.2	0.0	−35.8	−12.7
GMaS	0.3	−15.7	−12.8	0.3	−16.2	−15.5	0.0	−16.8	−17.7	1.7	−10.0	7.3
OI	17.4	−93.5	−94.4	5.5	−92.0	−92.3	0.5	−88.8	−88.7	8.1	−60.9	−56.5
OE	8.0	−112.1	−150.3	6.6	−108.9	−149.9	11.0	−103.6	−136.1	4.4	−83.7	−80.5
Pr	8.9	−69.0	−63.4	3.0	−66.0	−62.0	0.2	−60.7	−61.2	2.0	−45.1	−21.1
Ge	4.9	−92.8	−93.3	1.8	−93.1	−93.4	0.3	−96.3	−95.8	2.1	−60.1	−56.6
VLS	8.1	−170.7	−171.1	15.0	−171.0	−171.3	2.4	−171.1	−171.3	0.0	−170.3	−171.6
VLI	0.4	−172.0	−158.2	0.7	−172.5	−159.0	0.1	−172.6	−159.4	0.0	−171.1	−157.3
VI	2.4	−173.5	−168.6	4.5	−173.9	−168.9	0.7	−174.0	−169.1	0.0	−172.9	−169.2
VMI	2.5	−177.4	−155.9	4.6	−177.7	−156.9	0.8	−177.8	−157.7	0.0	−176.9	−154.1
VMS	1.5	−169.9	−166.4	2.7	−170.4	−166.8	0.4	−171.2	−167.0	0.0	−173.1	−166.7
AL	5.5	−20.5	13.1	5.8	−21.3	11.8	11.0	−22.4	10.0	0.4	−25.5	0.7
AB	2.6	−47.1	32.0	3.1	−47.3	28.0	6.4	−48.3	24.0	0.3	−59.6	11.4
AMD	0.1	−4.5	−0.8	1.0	−3.8	−2.7	3.0	−3.9	−4.0	0.0	−2.5	−8.1
AMM	0.0	−17.1	−12.1	0.1	−16.0	−14.8	0.2	−14.6	−12.9	0.0	−16.8	−17.7
AMP	0.1	−37.6	7.6	0.4	−39.8	−1.3	1.3	−39.6	−7.2	0.0	−41.5	−15.1
BF	2.1	−172.1	−178.4	0.4	−171.9	−176.5	1.8	−171.5	−174.5	4.0	−172.1	−178.1
PM	29.6	−13.2	34.2	14.1	−12.7	33.9	1.1	−15.8	35.8	10.2	−29.0	42.3
Il	10.9	−16.0	35.7	8.2	−15.8	35.8	11.9	−16.5	36.3	5.8	−27.3	41.6
GM	136.2	−170.4	−147.2	76.0	−170.8	−146.0	13.9	−169.1	−139.2	21.0	−170.2	−147.5
GL	53.7	−163.9	−118.8	31.0	−164.9	−118.6	4.5	−164.3	−116.9	0.0	−161.2	−117.4
Po	0.1	−118.0	−119.3	0.2	−113.5	−113.2	0.0	−105.1	−104.3	0.0	−81.9	−173.1
QF	1.6	−103.6	−175.3	1.5	−100.1	−161.3	2.4	−96.6	−134.4	0.4	−86.8	−80.9
Pe	1.7	−42.8	34.7	1.7	−43.1	33.6	3.1	−44.3	33.1	0.6	−55.2	29.9
Pl	1.3	−179.5	−164.1	0.9	−179.8	−155.2	0.1	−180.0	−149.1	0.0	−179.9	−167.6

a little later, at about 54%GC. The activity of *iliopsoas* was observed between 20%GC and 80%GC and both *iliacus* (Il) and *psoas* (PM) rather reciprocally complemented their actions. The activity of *adductors longus* and *brevis* (AL and AB) was visible between 35% GC and 80%GC, however, the maximum values of forces were much lower compared to the results obtained for the abductors. The activity of all parts of the *adductor magnus* (AMP, AMM, AMD) had a different course from the one described for other adductors with the highest force value observed during heel loading (4% GC). A similar situation was visible for both parts of the *gluteus maximus* (GMaI and GMaS). Significant values of muscular forces were observed at the beginning of the single support phase at 16%GC, especially for hip abductors. The second interesting point occurred at 47%GC when *gluteus medius* (anterior part) and *minimus* reached their maximum activity. The greatest muscular forces in the whole gait cycle were calculated for *gastrocnemius* with the

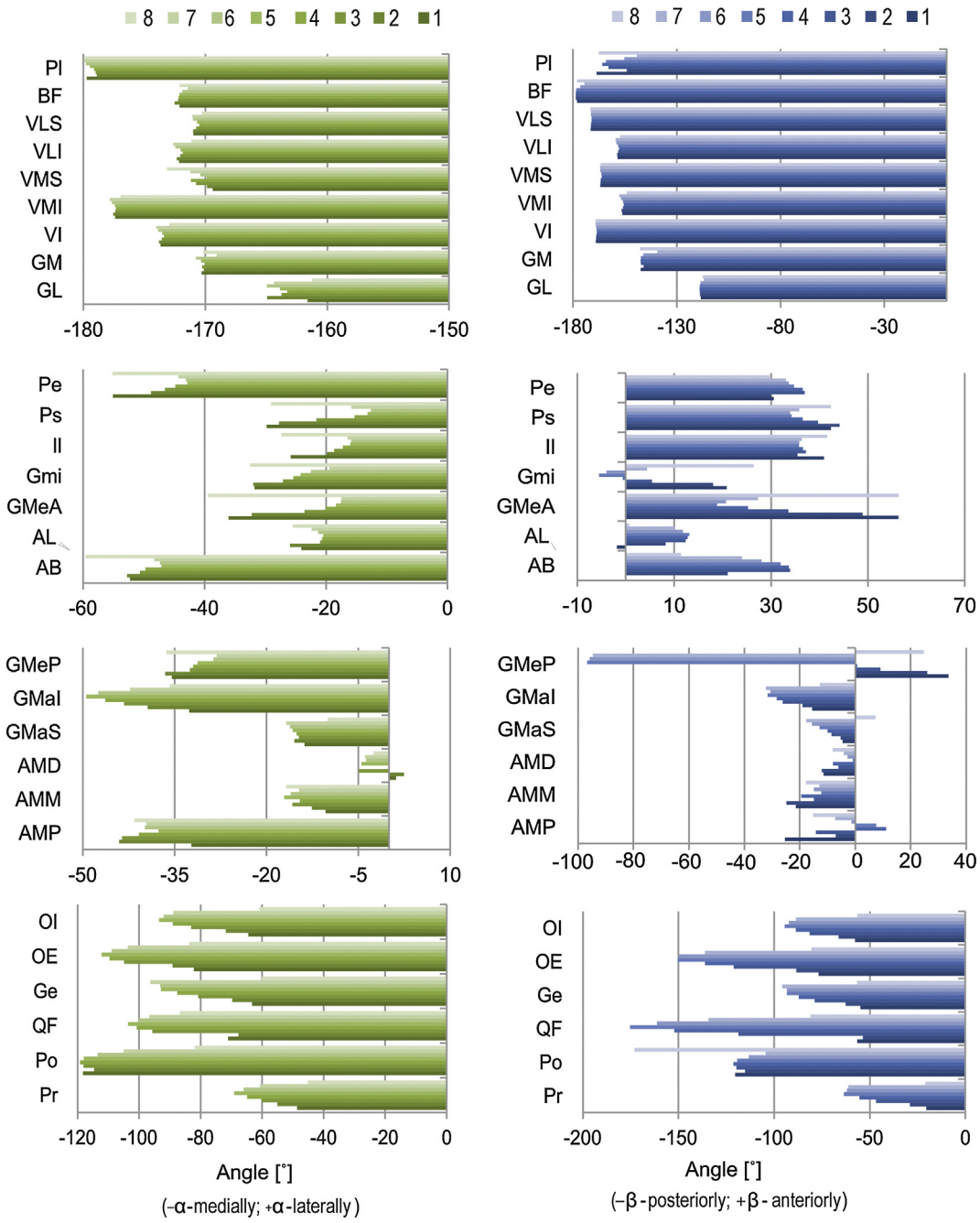

Fig. 5. The angles of the muscle force direction of 28 actons from the sagittal (-α - medially; +α - laterally) and coronal (-β - posteriorly; +β - anteriorly) planes of the femur for 8 time-points of the gait cycle (designation in Table 2 and Fig. 2).

maximum at the level of 136.3%BW for medial head and 53.7%BW for lateral head.

Force directions for all 28 actons is presented in Table 4 and in Fig. 5. It is worth mentioning that the line of muscle force vector in the femoral coordinate system remained almost constant during the whole gait cycle for some muscles (e.g. *vastus* muscles) whilst for others it was highly variable (e.g. GMeP). The variation range of the direction of force generated by individual muscles in the coronal and sagittal planes is presented in Fig. 6.

The coordinates of the muscular force vector attachment points on the femoral bone are presented in Table 5. They were determined as the average value for particular coordinates of all muscle parts of which the analysed acton was composed. The values presented refer to the geometry of the standard model available in the AnyBody system before scaling, with the length of the femur equal to 0.41 m. The way to determine the coordinates of the attachment points of particular muscles on the femoral bone for individual person is presented in Supplementary Material.

4. Discussion

The pattern of loadings acting on the femoral bone during normal gait was presented above. The hip-joint reaction force and the forces generated by muscles attached to the femur were determined using numerical simulation performed with the use of the

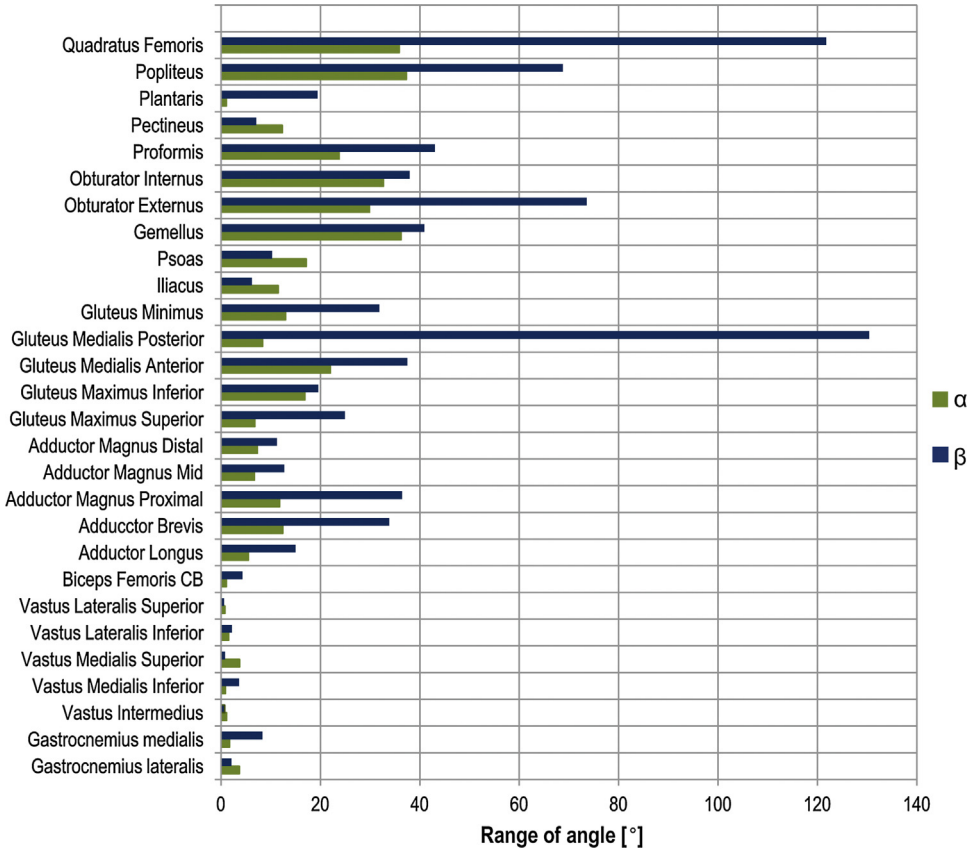

Fig. 6. The range of angles of deviation of the muscle forces direction (28 actons) from the sagittal (α) and coronal (β) planes of the femur.

AnyBody software and based on kinematic and kinetic data registered for a group of 99 young, healthy persons.

Two characteristic peaks in the hip-joint reaction force and many muscle forces and occurring at about 16%GC and 47%GC may be explained as a result of periodic acceleration and deceleration of the human body during the stance phase. The maximum values of resultant HJF presented in our study were higher than the results measured with the use of instrumented endoprosthesis by Davy et al. (1988) (266%BW) and Bergmann et al. (2001) (238% BW). However, it should be kept in mind that the results of abovementioned research were obtained for older persons after a total hip replacement, which could have affected the dynamics of locomotion. On the other side, the results obtained in numerical simulations (Thielen et al., 2009; Modenese et al., 2011) showed values of the joint reaction force at the same level as in our results (400% BW). Therefore, it can be noticed that usually *in-silico* analysis of the musculoskeletal system lead to overestimation of the joint reaction force value. This may be due to the fact that it is difficult to avoid same inaccuracy of the model, obtained by linear scaling of the generic model, comparing to characteristics of an individual patient (e.g. arms of muscle forces), simplifications of particular joints kinematics, etc. Accuracy of forces estimation can be improved by individual adjustment of the model to a specific patient, which requires usage of CT/MRI data (Marra et al., 2015; Jung et al., 2016; De Pieri et al., 2018). In our research, taking into account fact that a large group of healthy subjects was analysed, it was clearly impossible to incorporate such methodology.

The activity of particular muscles determined in the presented studies shows a high compliance with the results of electrical muscle activity (EMG) registered for healthy persons during gait (Wootten et al., 1990). Additionally, our results are very similar to those obtained by means of numerical simulation with the use of polynomial, third power muscle recruitment criterion by Lenaerts et al. (2008) and Modenese et al. (2011). Nevertheless, some discrepancies between our results and EMG observations were noted. The most predominant were visible in the case of *iliacus* and *psoas* as well as *adductor magnus* activity. In the first case, in EMG results, *iliacus* and *psoas* were usually treated as a unity (*iliopsoas*), whilst in our research both muscles were analysed separately. Their forces did not occur at the same time, but they reciprocally complement their activity, which may result from the optimisation procedure used in the research. According to EMG recordings, *adductor magnus* should be active at the end of the stance phase whilst in our results its greatest force was obtained at the beginning of the gait cycle, similarly to *gluteus maximus* and differently from other *adductors*. This result may be related to the role of *gluteus maximus* in maintaining (together with *adductor magnus*) the upright posture during locomotion (Wootten et al., 1990). Similar time characteristics of forces generated by both these muscles may be a proof of the validity of this thesis.

It is a well known fact that hip joint abductors play a special role in maintaining the equilibrium of the upper body part during the single support phase. The calculated resulting force of gluteus medius and minimus muscles acting in the coronal plane equal to 138%BW was higher than 104%BW, calculated for these muscles on the base of model of the lower extremity validated against in vivo data from walking and presented by Heller et al. (2005). However, it is known that the value of total abductor forces necessary to ensure the balance of the body during one-leg standing, taken from analytical studied of the static equilibrium conditions, is equal to 240%BW (Pauwels, 1976). A stabilizing influence on the pelvis of *tensor fasciae latae* and *ilio-tibial tract* which were omitted in the

Table 5
Coordinates (m) of attachment points to the femur of 28 actons in the standard AnyBody model, for femoral bone length of 0.41 m.

Acton	Coordinates (m)			Acton	Coordinates (m)		
	X_{MODEL}	Y_{MODEL}	Z_{MODEL}		X_{MODEL}	Y_{MODEL}	Z_{MODEL}
Gluteus Medius Posterior	−0.042	0.007	0.043	Adductor Longus	0.023	−0.205	0.014
Gluteus Medius Anterior	−0.025	−0.009	0.063	Adductor Brevis	−0.009	−0.114	0.019
Gluteus Minimus	−0.015	−0.023	0.062	Adductor Magnus Distal	0.057	−0.363	−0.025
Gluteus Maximus Inferior	0.006	−0.170	−0.010	Adductor Magnus Middle	0.026	−0.230	0.011
Gluteus Maximus Superior	−0.009	−0.114	−0.010	Adductor Magnus Proximal	0.008	−0.138	0.015
Obturator Internus	−0.027	−0.003	0.040	Biceps Femoris Caput Brevis	0.017	−0.239	0.016
Obturator Externus	−0.037	−0.029	0.026	Psoas Major	−0.023	−0.070	0.004
Piriformis	−0.035	0.009	0.027	Iliacus	−0.023	−0.070	0.004
Gemellus	−0.027	0.003	0.040	Gastrocnemius Medialis	0.050	−0.367	−0.015
Vastus Lateralis Superior	−0.018	−0.022	0.056	Gastrocnemius Lateralis	0.034	−0.378	0.022
Vastus Lateralis Inferior	0.002	−0.182	0.029	Popliteus	0.027	−0.411	0.045
Vastus Intermedius	0.032	−0.175	0.036	Quadratus Femoris	−0.046	−0.036	0.029
Vastus Medialis Superior	0.016	−0.140	0.024	Pectineus	−0.017	−0.083	0.016
Vastus Medialis Inferior	0.045	−0.271	0.010	Plantaris	0.028	−0.386	0.037

present study as both these structures have no direct attachments to the femoral bone should also be kept in mind. The muscle force of hip abductors deviated from the vertical line in the medial direction by an angle in the range of 20–41°. It is similar to results obtained by other authors: 30–35° (Heller et al., 2001; Heller et al., 2005), 20–36° (Yadav et al., 2016), 25–48° (Bitsakos et al., 2005). In general, the force vectors for a majority of muscles were directed proximally, medially and posteriorly (with the exception of *vastus muscles* and *gastrocnemius*). This was not surprising when we take into account the location of particular muscles against the femoral bone.

The variability of the muscle force direction during the gait cycle reflected the movement of particular muscles in relation to the femur. The range of such effect varied for particular muscles, but for most of them the change of the angles of deviation of the force from the coronal plane of the femur (β) was greater than from the sagittal plane of the femur (α). The range of variation of the β angle is usually in the interval of 20–40° whilst in the case of the α angle the changes in its value were in the range of 10–20°. An almost stable direction of the muscle forces during the whole gait cycle was observed for *vastus muscles*, *gastrocnemius* and *biceps femoris caput breve*. In contrast, a great variability of the force direction was observed for the posterior part of *gluteus medius*, with a transition from the anterior to the posterior direction. Similar results were presented by Heller et al. (2001), Yadav et al. (2016) and Campoli et al. (2012).

It should also be noted that the present study was performed only for the preferred speed, neglecting the influence of gait velocity. Controversies may also concern the method of division of the whole muscles into actons. Such a dilemma concerns, among others, *gluteus minimus*. In the present study, taking into account a small area of attachment on the greater trochanter and a high level of coherence in directions of forces generated by particular muscle parts, *gluteus minimus* was treated as a single muscle. However, sometimes *gluteus minimus* was divided into two or even three parts (Yadav et al., 2016).

The calculation of forces acting in the musculoskeletal system with the use of inverse dynamics and optimization method are susceptible to some errors characteristic for this methodology, such as soft-tissue artefacts or errors occurring when converting the motion capture data to a model. Moreover, the presented model of loadings acting on the femoral bone is worth improving in future research by including forces generated by those muscles which influence the femoral bone (e.g. *rectus femoris* or *tensor fasciae latae*), even though they have no direct attachments on this bone.

5. Conclusions

The pattern of loadings acting on the femoral bone during normal gait, obtained by modelling and computer simulation performed with the use of the AnyBody system and based on kinematic and kinetic data registered for ninety-nine healthy people, was the main result of the present research. Force values and directions, variable during the gait cycle, were presented for the hip-joint reaction as well as for muscles attached to the femoral bone. A similar analysis for other bones like tibia, pelvis, lumbar vertebras should be conducted in the future.

Acknowledgments

The research was conducted as a part of the Projects MB/WM/14/2018 and S/WM/1/2017 and financed with the use of funds for science from the Polish Ministry of Science and Higher Education.

Conflict of interest statement

No conflict of interest to report.

Appendix A. Supplementary material

Supplementary data to this article can be found online at https://doi.org/10.1016/j.jbiomech.2019.02.018.

References

Bergmann, G., Deuretzbacher, G., Heller, M., Graichen, F., Rohlmann, A., Strauss, J., Duda, G.N., 2001. Hip contact forces and gait patterns from routine activities. J. Biomech. 34, 859–871.
Bitsakos, C., Kerner, J., Fisher, I., Amis, A.A., 2005. The effect of muscle loading on the simulation of bone remodelling in the proximal femur. J. Biomech. 38, 133–139.
Campoli, G., Weinans, H., Zadpoor, A.A., 2012. Computational load estimation of the femur. J. Mech. Behav. Biomed. Mater. 10, 108–119.
Carter, D.R., van der Meulen, M.C.H., Beaupre, G.S., 1996. Mechanical factors in bone growth and development. Bone 18, 5S–10S.
Cowin, S.C., Hegadus, D.H., 1976. Bone remodeling I: theory of adaptive elasticity. J. Elast. 6, 313–326.
Damsgaard, M., Rasmussen, J., Soren, T.C., Surma, E., de Zee, M., 2006. Analysis of musculoskeletal systems in the AnyBody modeling system. Simul. Model. Pract. Theory 14, 1100–1111.
Davis, R.B., Ounpuu, S., Tyburski, D., Gage, J.R., 1991. A gait data collection and reduction technique. Human Movement Sci. 10, 575–587.
Davy, D.T., Kotzar, G.M., Brown, R.H., Heilple, K.G., Goldberg, V.M., Heiple, K.G.J.R., Berilla, J., Burstein, A.H., 1988. Telemetric force measurements across the hip after total arthroplasty. J. Bone Joint Surg. American 70 (1), 45–50.

De Pieri, E., Lund, M.E., Gopalakrishnan, A., Rasmussen, K.P., Lunn, D.E., Ferguson, S. J., 2018. Refining muscle geometry and wrapping in the TLEM 2 model for improved hip contact force prediction. PLoS One 13, e0204109.
Duda, G.N., 1996. Influence of muscle forces on the internal loading in the femur during gait Ph.D. thesis. Technical University Hamburg-Harburg, Hamburg and Shaker Verlag, Aachen.
Duda, G.N., Heller, M., Albinger, J., Schulz, O., Schneider, E., Claes, L., 1998. Influence of muscle forces on femoral strain distribution. J. Biomech. 31 (9), 841–846.
Erdemir, A., McLean, S., Herzog, V., van den Bogert, A.J., 2007. Model-based estimation of muscle forces exerted during movements. Clin. Biomech. 22, 131–154.
Heinen, F., Lund, M.E., Rasmussen, J., de Zee, M., 2016. Muscletendon unit scaling methods of Hill-type musculoskeletal models: An overview. In: Proceedings of the Institution of Mechanical Engineers part H: Journal of Engineering in Medicine 230(10), 976–984.
Heller, M.O., Bergmann, G., Deuretzbacher, G., Dürselen, L., Pohl, M., Claes, L., et al., 2001. Musculo-skeletal loading conditions at the hip during walking and stair climbing. J. Biomech. 34 (7), 883–893.
Heller, M.O., Bergmann, G., Kassi, J.-P., Claes, L., Haas, N.P., Duda, G.N., 2005. Determination of muscle loading at the hip joint for use in pre-clinical testing. J. Biomech. 38 (5), 1155–1163.
Jang, I.G., Kim, I.Y., 2009. Computational simulation of trabecular adaptation progress in human proximal femur during growth. J. Biomech. 42, 573–580.
Jonkers, I., Sauwen, N., Lenaerts, G., Mulier, M., Perre, G.V., Jaecques, S., 2008. Relation between subject-specific hip joint loading, stress distribution in the proximal femur and bone mineral density changes after total hip replacement. J. Biomech. 41, 3405–3413.
Jung, Y., Phan, C., Koo, S., 2016. Intra-articular knee contact force estimation during walking using force-reaction elements and subject-specific joint model. J. Biomech. Eng. 138, (2). https://doi.org/10.1115/1.4032414 021016.
Klein-Horsman, M.D., Koopman, H.F., van der Helm, F.C., Prosé, L.P., Veeger, H.E., 2007. Morphological muscle and joint parameters for musculoskeletal modelling of the lower extremity. Clin. Biomech. 22, 239–247.
Lenaerts, G., Groote, F. De, Demeulenaere, B., Mulier, M., van der Perre, G., Spaepen, A., Jonkers, I., 2008. Subject-specific hip geometry affects predicted hip joint contact forces during gait. J. Biomech. 41, 1243–1252.
Lund, M.E., Andersen, M.S., de Zee, M., Rasmussen, J., 2015. Scaling of musculoskeletal models from static and dynamic trials. Int. Biomech. 2 (1), 1–11.
Machado, M.M., Fernandes, P.R., Zymbal, V., Baptista, F., 2014. Human proximal femur bone adaptation to variations in hip geometry. Bone 67, 193–199.
Marra, M., Vanheule, V., Fluit, R., Koopman, B.H.F.J.M., Rasmussen, J., Verdonschot, N., Andersen, M.S., 2015. A subject-specific musculoskeletal modeling framework to predict in vivo mechanics of total knee arthroplasty. J. Biomech. Eng. 137, (2). https://doi.org/10.1115/1.4029258 020904.
Märdian, S., Schaser, K.D., Duda, G.N., Heyland, M., 2015. Working length of locking plates determines interfragmentary movement in distal femur fractures under physiological loading. Clin. Biomech. 30 (4), 391–396.
Modenese, L., Phillips, A.T.M., Bull, A.M.J., 2011. An open source lower limb model: hip joint validation. J. Biomech. 44 (12), 2185–2193.
Niinimäki, S., Narra, N., Härkönen, L., Abe, S., Nikander, J., Hyttinen, J., Knüsel, C., Sievänen, H., 2017. The relationship between loading history and proximal femoral diaphysis cross-sectional geometry. American J. Human Biol. 2017, (29). https://doi.org/10.1002/ajhb.22965 e22965.
Pauwels, F., 1976. Biomechanics of the normal and diseased hip - An atlas. Springer-Verlag, Berlin Heidelberg.
Prendergast, P.J., 2002. Mechanics applied to skeletal ontogeny and phylogeny. Meccanica 37, 317–334.
Piszczatowski, S., 2008. Analysis of the stress and strain in hip joint of the children with adductors spasticity due to cerebral palsy. Acta Bioeng. Biomech. 10, 51–56.
Prilutsky, B.I., Gregor, R.J., 2000. Analysis of muscle coordination strategies in cycling. IEEE Trans. Rehabilit. Eng. 8 (3), 362–370.
Prilutsky, B.I., Zatsiorsky, V.M., 2002. Optimization-based models of muscle coordination. Excercise Sport Sci. Rev. 30 (1), 32–38.
Rasmussen, J., de Zee, M., Damsgaard, M., Christensen, S.T., Marek, C., Siebertz, K., 2005. A general method for scaling musculo-skeletal models. International Symposium on Computer Simulation in Biomechanics, Cleveland, OH.
Rauch, F., 2005. Bone growth in length and width: the Yin and Yang of bone stability. J. Musculoskeletal Neuronal Interact 5 (3), 194–201.
Seo, J.W., Kang, D.W., Kim, J.Y., Yang, S.T., Kim, D.H., Choi, J.S., Tack, G.R., 2014. Finite element analysis of the femur during stance phase of gait based on musculoskeletal model simulation. Bio-Med. Mater. Eng. 24, 2485–2493.
Thielen, T., Maas, S., Zürbes, A., Waldmann, D., Kelm, J., 2009. Entwicklung einer Hüftinterimsprothese mittels FE-Analyse unter Berücksichtigung der Muskel- und Gelenkkräfte aus AnyBody,Ansys Conference & 27th CADFEM Users' Meeting 2009, Germany.
Wootten, M., Kadaba, M., Cochran, G., 1990. Dynamic electromyography. II. Normal patterns during gait. J. Orthop. Res. 8, 259–265.
Wu, G., Siegler, S., Allard, P., Kirtley, C., Leardini, A., Rosenbaum, D., Whittle, M., D'Lima, D.D., Cristofolini, L., Witte, H., Schmid, O., Stokes, I., 2002. ISB recommendation on definitions of joint coordinate system of various joints for the reporting of human joint motion-part I: ankle, hip, and spine. Int. Soc. Biomech., J. Biomech. 35 (4), 543–548.
Yadav, P., Shefelbine, S.J., Gutierrez-Farewik, E.M., 2016. Effect of growth plate geometry and growth direction on prediction of proximal femoral morphology. J. Biomech. 49 (9), 1613–1619.